

## Cyclooxygenase-2 in Human and Experimental Ischemic Proliferative Retinopathy

F. Sennlaub, MD, PhD; F. Valamanesh, MSc; A. Vazquez-Tello, PhD; A.M. El-Asrar, MD, PhD; D. Checchin, MSc; S. Brault, MSc; F. Gobeil, PhD; M.H. Beauchamp, MSc; B. Mwaikambo, BSc; Y. Courtois, PhD; K. Geboes, MD, PhD; D.R. Varma, MD, PhD; P. Lachapelle, PhD; H. Ong, PhD; F. Behar-Cohen, MD, PhD; S. Chemtob, MD, PhD



**Background**—Intravitreal neovascular diseases, as in ischemic retinopathies, are a major cause of blindness. Because inflammatory mechanisms influence vitreal neovascularization and cyclooxygenase (COX)–2 promotes tumor angiogenesis, we investigated the role of COX-2 in ischemic proliferative retinopathy.

**Methods and Results**—We describe here that COX-2 is induced in retinal astrocytes in human diabetic retinopathy, in the murine and rat model of ischemic proliferative retinopathy in vivo, and in hypoxic astrocytes in vitro. Specific COX-2 but not COX-1 inhibitors prevented intravitreal neovascularization, whereas prostaglandin E<sub>2</sub>, mainly via its prostaglandin E receptor 3 (EP<sub>3</sub>), exacerbated neovascularization. COX-2 inhibition induced an upregulation of thrombospondin-1 and its CD36 receptor, consistent with the observed antiangiogenic effects of COX-2 inhibition; EP<sub>3</sub> stimulation reversed effects of COX-2 inhibitors on thrombospondin-1 and CD36.

**Conclusion**—These findings point to an important role for COX-2 in ischemic proliferative retinopathy, as in diabetes. (*Circulation*. 2003;108:198-204.)

**Key Words:** prostaglandins ■ diabetes mellitus ■ ischemia ■ vasculature

Intravitreal neovascularization, which characterizes diabetic retinopathy, retinopathy of prematurity, or retinal vein occlusion, is a major cause of blindness.<sup>1</sup> Retinal ischemia is a common precursor to vitreal neovascularization in retinal diseases<sup>2</sup> and is associated with a local inflammatory response in the ischemic retina.<sup>3</sup> Early proinflammatory genes are expressed in ischemic disorders. We have recently shown that inducible NO synthase contributes to the development of intravitreal neovascularization<sup>4</sup> and to retinal apoptosis and degeneration.<sup>5</sup>

Cyclooxygenase (COX)-2 is also an immediate-early gene product of inflammation.<sup>6</sup> Prostanoids are synthesized principally via activities of COX-1 and COX-2. COX-1 is mostly constitutive and is expressed in most tissues. COX-2 is induced by cytokines, mitogens, and endotoxins, accounting for elevated prostaglandin production during inflammation.<sup>6</sup>

COX-2 can be expressed developmentally and on ischemic stimuli in retina.<sup>7</sup> COX-2 exerts an angiogenic effects in tumors<sup>8,9</sup> and in corneal neovascularization.<sup>10</sup> It has also been shown that prostanoids, notably prostaglandin E<sub>2</sub> (PGE<sub>2</sub>), stabilize the hypoxia-inducible factor<sup>11</sup> and stimulate expres-

sion of basic regulators of angiogenesis, including vascular endothelial growth factor (VEGF) in tumor endothelium,<sup>8</sup> resulting in endothelial cell proliferation.<sup>12</sup> We hereby investigated the role of COX-2 in a nontumoral condition, namely ischemic proliferative retinopathy, using human retinal tissue and experimental proliferative ischemic retinopathy. Our findings disclose an important role for this immediate-early gene product in proliferative retinopathy mediated (at least in part) by PGE<sub>2</sub> mostly via prostaglandin E receptor 3 (EP<sub>3</sub>) through a previously undescribed action involving thrombospondin-1 (TSP-1) and CD36.

### Methods

#### Human Samples

The eyes from 7 postmortem humans with diabetes mellitus, 4 eyes from 4 postmortem humans with no history of diabetes or ocular disease, and the ipsilateral eye from 1 subject with ocular ischemic syndrome secondary to severe carotid artery obstruction (case 12) were obtained.

Received March 10, 2003; revision received May 20, 2003; accepted May 20, 2003.

From the Departments of Pediatrics, Ophthalmology, and Pharmacology, Research Center of Hôpital Sainte-Justine (F.S., A.V.-T., D.C., S.B., F.G., M.H.B., B.M., S.C.); Departments of Pharmacology (D.R.V., B.M.) and Ophthalmology (P.L.), McGill University; and Faculty of Pharmacy, Université de Montréal (H.O.), Montreal, Québec, Canada, and Développement, Vieillesse et Pathologie de la Rétine, Institut National de la Santé et de la Recherche Médicale U450, Paris, France (F.V., Y.C., F.B.C.); Department of Ophthalmology, College of Medicine, King Saud University, Riyadh, Saudi Arabia (A.M.E.-A.); and Department of Pathology, University Hospitals Leuven, Belgium (K.G.).

This article originally appeared Online on June 23, 2003 (*Circulation*. 2003;107:r126–r132).

Correspondence to Florian Sennlaub, MD, PhD, Department of Pediatrics, Centre de Recherche, Hôpital Sainte-Justine, 3175, chemin de la Côte-Sainte-Catherine, Montréal, Québec, Canada H3T 1C5. E-mail fsennlaub@justine.umontreal.ca

© 2003 American Heart Association, Inc.

*Circulation* is available at <http://www.circulationaha.org>

DOI: 10.1161/01.CIR.0000080735.93327.00

## Subject Characteristics and Results of COX-2 Staining

Case No.	Age, Sex	Type of DM	Duration of DM, y	Cause of Death	Death to Enucleation, h	COX-2 Expression in NFL
Subjects with diabetes						
1	52, M	IDDM	14	Coronary artery disease	14	+
2	68, M	NIDDM	15	Intestinal ischemia	6	+
3	75, F	NIDDM	14	Coronary artery disease	17	+
4	74, F	NIDDM	10	Chronic obstructive pulmonary disease	12	+
5	70, M	NIDDM	20	Renal failure	9	+
6	58, M	NIDDM	16	Intracranial bleeding	10	+
7	67, F	NIDDM	18	Coronary artery disease	21	+
Subjects without diabetes						
8	37, F	...	...	Cardiogenic shock	12	—
9	52, M	...	...	Colorectal cancer	17	—
10	78, M	...	...	Chronic obstructive lung disease	17	—
11	41, M	...	...	Road traffic accident	15	—
12	41, M	...	...	Road traffic accident	17	+

DM indicates diabetes mellitus; IDDM, insulin-dependent diabetes mellitus; NIDDM, non-insulin-dependent diabetes mellitus; NFL, nerve fiber layer; M, male; and F, female.

## Animal Models of Ischemic Proliferative Retinopathy

All procedures were conducted in accordance with the Association for Research in Vision and Ophthalmology's statement, *The Use of Animals in Ophthalmic and Vision Research*.

In the murine model, C57BL/6 mice at postnatal day (P) 7 were exposed, with their mothers, for 5 days to hyperoxic conditions (75% O<sub>2</sub>), inducing vaso-obliteration of the central retinal vasculature.<sup>13</sup> At P12, mice were returned to room air; extensive vitreal neovascularization was present in all mice, with the maximum effect observed on P17. Ischemic proliferative retinopathy was also reproduced in Sprague-Dawley rats exposed to 7 cycles of hyperoxia (80% O<sub>2</sub>, 20.5 hours) and hypoxia (10% O<sub>2</sub>, 0.5 hours) with a gradual return to 80% O<sub>2</sub> over 3 hours, from P1 to P7.<sup>14</sup> Thereafter, rats were returned to room air, and neovascularization was evaluated at P12.

Mice and rats were anesthetized with an intraperitoneal injection of a ketamine (100 mg/kg) and xylazine (15 mg/kg) solution and intravitreally injected using glass capillaries ( $\approx 60$  gauge). Right eyes of mice were injected intravitreally at P13 and P15 with 0.5  $\mu$ L of vehicle (50% polyethylene glycol [Sigma-Aldrich], 40% PBS, and 10% ethanol); 2, 10, or 50  $\mu$ mol/L of specific COX-2 inhibitor o-(Acetoxyphenyl)hept-2-ynyl sulfide (APHS)<sup>15</sup> (Calbiochem, France Biochem) (n=16/group); vehicle (90% 0.9% NaCl and 10% ethanol); 2, 10, or 50  $\mu$ mol/L of the selective COX-1 inhibitor SC-560<sup>16</sup> (Calbiochem) (n=16/group); or 0.3  $\mu$ mol/L 16,16-dimethyl-PGE<sub>2</sub> (Sigma-Aldrich), resulting in estimated effective vitreal concentrations of drugs (estimated total eye volume of 10  $\mu$ L based on spheric volume and volume-to-weight ratio calculation) of 0.2, 1, and 5  $\mu$ mol/L (APHS and SC-560) and 0.03  $\mu$ mol/L (16,16-dimethyl-PGE<sub>2</sub>). Eyes were enucleated at P17 and subjected to retinal histochemistry (n=8) and intravitreal neovascularization quantification (n=8) (see below). Rat pups (n=8 to 13/group) were injected in the right eye at P7 and P9 with either 1  $\mu$ L of vehicle (NaCl 0.9%) or the selective COX-2 inhibitor etodolac 40  $\mu$ mol/L<sup>16</sup> (Sigma-Aldrich) with or without 16,16-dimethyl-PGE<sub>2</sub> 4  $\mu$ mol/L (Cayman Chemicals), a specific EP<sub>2</sub> or EP<sub>3</sub> agonist, respectively, butaprost 400  $\mu$ mol/L (Cayman Chemicals) or M&B28767 4  $\mu$ mol/L (Rhone-Poulenc Rorer),<sup>17</sup> to obtain estimated effective vitreal concentrations of drugs (estimated total eye volume of 40  $\mu$ L) of 1 (etodolac), 0.1 (16,16-dimethyl-PGE<sub>2</sub>), 10 (butaprost), and 0.1 (M&B28767)  $\mu$ mol/L; EP<sub>2</sub> and EP<sub>3</sub> receptor agonists were used because antagonists are not readily available. Rats were euthanized at P12 and retinas stained for endothelial cells and flat mounted (see below).

## Immunohistochemistry

Human and murine eyes were fixed in 4% paraformaldehyde and embedded, sectioned (5  $\mu$ m), and deparaffinized. Sections were stained using a heat-induced antigen retrieval and a 3-step avidin-biotin complex technique using avidin-alkaline phosphatase or avidin-FITC as previously described.<sup>4</sup> Antibodies used were polyclonal COX-2 antibody (Biomol Laboratories and Cayman Chemical Co), monoclonal EP<sub>3</sub> antibody (generous donation by Exalpa Biologicals), monoclonal glial fibrillary acidic protein (GFAP) (Oncogene), and TRITC-conjugated lectin griffonia simplicifolia (Sigma-Aldrich).

## Cell Culture

Given the need for sufficient tissue quantities, primary astrocyte and endothelial cell cultures were obtained for practical reasons from neonatal porcine retinas; cells from this species respond to a variety of stimuli implicated in ischemic retinopathies in the same manner as that of rodent tissues.<sup>18,19</sup> Neonatal porcine retinal astrocytes were isolated as described for brain astrocytes.<sup>20</sup> Cells of the third to fourth passages were used. Cultures were  $\approx 95\%$  GFAP positive. Monolayers (80% confluent) of astrocytes were incubated at 37°C either under normoxic (95% air, 5% CO<sub>2</sub>) or hypoxic conditions (2% O<sub>2</sub>, 5% CO<sub>2</sub>, 93% N<sub>2</sub>) for 24 hours. Subsequently, the medium was changed and cells were incubated for 1 hour in the presence of APHS (1  $\mu$ mol/L), etodolac (1  $\mu$ mol/L), SC-560 (0.2  $\mu$ mol/L), or etodolac (1  $\mu$ mol/L) and SC-560 (0.2  $\mu$ mol/L); drug concentrations used were equivalent to those estimated in vivo. PGE<sub>2</sub> concentrations were measured in the supernatant, and the cells were harvested for protein quantification and Western blot analysis. The pH of the medium was unchanged during 24-hour hypoxia. For endothelial cell culture, newborn porcine neuroretinal microvessels were isolated as previously reported.<sup>18</sup>

## Western Blot

Protein extraction of cells was performed as previously described.<sup>18</sup> Rat retinas were pooled<sup>3,4</sup> and membranous and cytosolic fractions were separated as previously described.<sup>21</sup> Antibodies used were polyclonal anti-COX-2 (Cayman); polyclonal anti-COX-1 (Santa Cruz Biotechnology); mouse monoclonal EP<sub>2</sub>, EP<sub>3</sub>, and EP<sub>4</sub> (Exalpa Biologicals); polyclonal anti-VEGF antibody (Chemicon); rat monoclonal anti-VEGF receptor (VEGFR)-2 (Chemicon); monoclonal anti-TSP-1 (Oncogene); polyclonal purified anti-CD36; monoclonal

anti-clathrin (Transduction Laboratories, BD Biosciences); monoclonal anti- $\beta$ -actin (Novus Biological); and monoclonal GFAP (Onco-gene). Western blots were performed on equal amounts of proteins as described.<sup>18</sup>

### PGE<sub>2</sub> Radioimmunoassay

PGE<sub>2</sub> concentrations in retinal tissue (n=3 per group) and astrocyte supernatant were determined as previously described.<sup>22</sup>

### RNA Isolation and Reverse Transcription–Polymerase Chain Reaction (PCR) Analysis

Retinal mRNA expression from whole retinal extracts (n=3 per group) was analyzed using reverse transcription–PCR (cycles below the saturating conditions) as previously described.<sup>4</sup> Oligonucleotide primers were the following: for COX-2, antisense 5'-GGAGAAGGCTTCCCAGCTTTTG-3', and sense 5'-GCAAATCCTTGCTGTTCCAATC-3', resulting in a PCR product of 336 bp; for actin, antisense 5'-GCTCATGCGGATAGTGATGACCT-3', and sense 5'-GGTGGGTATGGGT-CAGAAGGA-3', resulting in a 630-bp PCR product.

### Quantification of Vitreal Neovascularization and Intraretinal Revascularization

Mouse eyes were paraffin embedded, cut sagittally (parallel to the optic nerve), and stained with periodic acid-Schiff and Hemalun. Vitreal neovascularization (vascular cell nuclei found on the vitreal side of the inner limiting membrane) was counted by blinded investigators as previously described.<sup>4</sup> Neovascular nuclei were absent in animals raised in room air. Intraretinal vasculature was visualized on retinal flat mounts stained with TRITC-conjugated lectin griffonia simplicifolia (Sigma-Aldrich),<sup>23</sup> and the surface of the capillary free area measured using a computerized image-analysis system (Scion Image). In the rat model, intravitreal neovascularization was evaluated by counting intravitreal neovascular tufts on lectin-stained retinal flat mounts.

### Statistical Analysis

Results are expressed as mean $\pm$ SEM. Statistical analyses were performed using the Mann-Whitney test and ANOVA. Statistical significance was set at  $P<0.05$ .

## Results

### COX-2 Expression in Human Diabetic Retina

Patient characteristics are summarized in the Table. COX-2 immunoreactivity was observed in all eyes in the retinal pigment epithelial cells, in the outer segment of the photoreceptors and to some degree in the inner plexiform layer (data not shown). In all diabetic subjects, COX-2 immunoreactivity was also detected in the nerve fiber layer (NFL) (Figure 1a, cases 1 to 7); this COX-2 immunostaining was granular and discontinuous. COX-2 immunolocalized mostly with GFAP indicative of astrocytes (Figure 1c through 1e); similar results were obtained using 2 different COX-2-specific antibodies (see Methods). A comparable pattern was found in the eye of a nondiabetic subject who had suffered from severe carotid artery obstruction (case 12). In contrast, in the other nondiabetic patients, COX-2 immunoreactivity was not observed in the NFL (Figure 1b and 1f through 1h, cases 8 to 11).

### COX-2 Expression and Localization, and PGE<sub>2</sub> Concentrations in Experimental Ischemic Retinopathy

COX-2 expression is altered by ischemia in neural tissue.<sup>24</sup> We explored the involvement of COX-2 in a murine model of retinopathy of prematurity. Equivalent COX-2 mRNA ex-

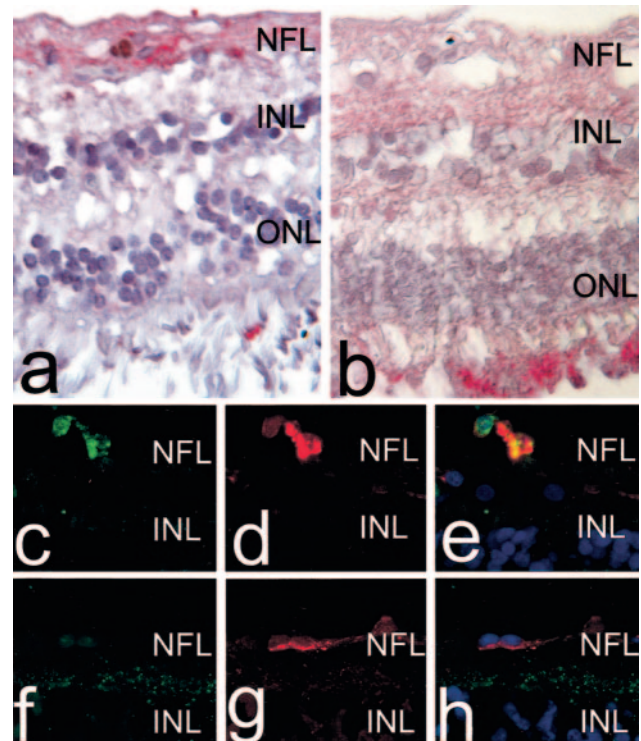


**Figure 1.** COX-2 immunohistochemistry on human retinas of diabetic (a and c through e) and nondiabetic (b and f through h) subjects. Shown is colocalization of GFAP and COX-2 in nondiabetic (f through h) and diabetic (c through e) eyes. Panel heights are 240  $\mu$ m (a and b) and 90  $\mu$ m (c through h). NFL indicates nerve fiber layer; INL and ONL, inner nuclear layer and outer nuclear layer, respectively.

pression was observed in room air and after hyperoxia exposure at P12, P14, and P17 (Figure 2A). Immunolocalization of COX-2 was studied in mouse retina and was found to be similar to that in humans. In normoxic mice at P14, COX-2 protein was robustly expressed in retinal pigment epithelial cells both in the outer photoreceptor segment and in the inner plexiform layer (data not shown). In the post-hyperoxia-exposed retinas, COX-2 expression was also detected in the NFL at P14 (Figure 3a) predominantly in astrocytes (GFAP positive) (Figure 3e and 3f).

COX-2 protein expression was evaluated in membrane fractions of retina extracts from hyperoxia-exposed rats. At the end of the hyperoxic period (P1 through P7), COX-2 immunoreactivity diminished and tended to increase in the early hours after resuming exposure to room air (24 hours after hyperoxia; Figure 2C). COX-1 exhibited the reverse pattern, and consequently whole retina concentrations of PGE<sub>2</sub>, a mediator involved in angiogenesis,<sup>25</sup> were unaltered during the posthyperoxia period (Figure 2B); although this does not exclude a local paracrine effect of this autacoid. Consistent with these observations, primary retinal astrocyte cultures exposed for 24 hours to relative hypoxia (2% O<sub>2</sub>, 5% CO<sub>2</sub>, 93%) exhibited increased COX-2 expression (Figure 2D) and PGE<sub>2</sub> levels (Figure 2E) compared with those in normoxia (95% air, 5% CO<sub>2</sub>), whereas COX-1 expression remained steady. Specific COX-2 inhibitors, APhS and etodolac, markedly dimin-



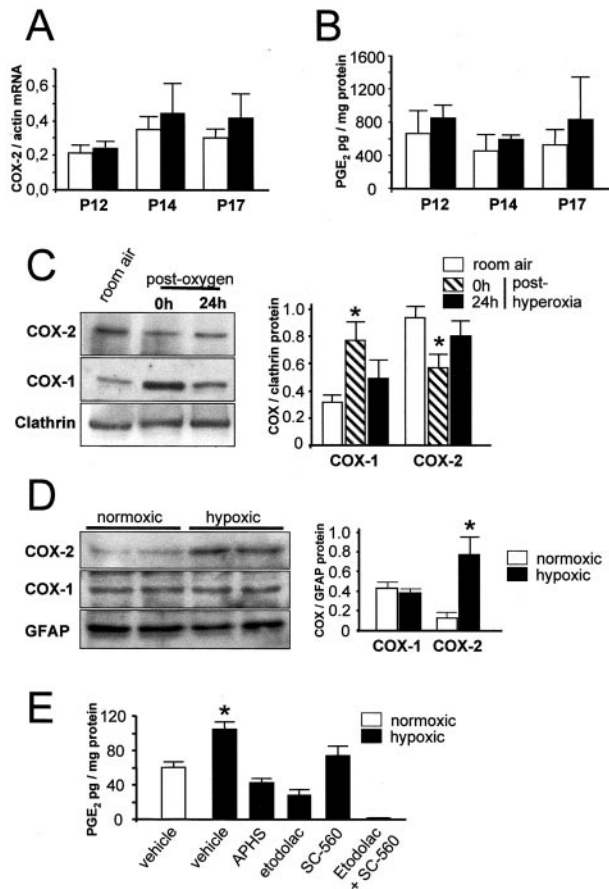


**Figure 2.** COX expression and PGE<sub>2</sub> levels in retina of models of ischemic proliferative retinopathy. Mice were exposed to 75% O<sub>2</sub> from P5 to P12, and rats to cycling O<sub>2</sub> concentrations of 10% to 80% from P1 to P7. A, COX-2 mRNA expression in mice. B, Retinal PGE<sub>2</sub> concentrations in mice. C, COX-1 and -2 immunoreactivity in rats. D, COX-1 and -2 immunoreactivity in cultured astrocytes in 21% or 2% O<sub>2</sub> for 24 hours (see Methods). E, PGE<sub>2</sub> levels in media of cultured astrocytes in normoxic (20% O<sub>2</sub>) and hypoxic (2% O<sub>2</sub>) conditions with or without 1-hour treatment with APHS (1  $\mu$ mol/L), etodolac (1  $\mu$ mol/L), and/or SC-560 (0.2  $\mu$ mol/L). Histogram bar values are mean  $\pm$  SEM. \* $P$  < 0.05 compared with other corresponding values.

ished PGE<sub>2</sub> levels, whereas COX-1-selective SC-560 only caused a small decrease in PGE<sub>2</sub> concentrations (Figure 2E) even at highest dose tested (5  $\mu$ mol/L), suggesting a dominant role for COX-2 in PGE<sub>2</sub> generation during hypoxia.

In age-adjusted normoxic whole retinas, COX-1 and -2 expression did not change. Immunolocalization of COX-2 in rat retina was similar to that observed in mouse (data not shown).

### COX Inhibition in Ischemic Proliferative Retinopathy

The impact of COX inhibition on neovascularization was tested using specific COX-2 (APHS and etodolac) and COX-1 (SC-560) inhibitors; concentrations corresponded to effective ones on astrocyte PGE<sub>2</sub> levels (Figure 2E). In vivo, posthyperoxia administration of the preferential COX-2 inhibitor APHS did not affect the degree of capillary-free area

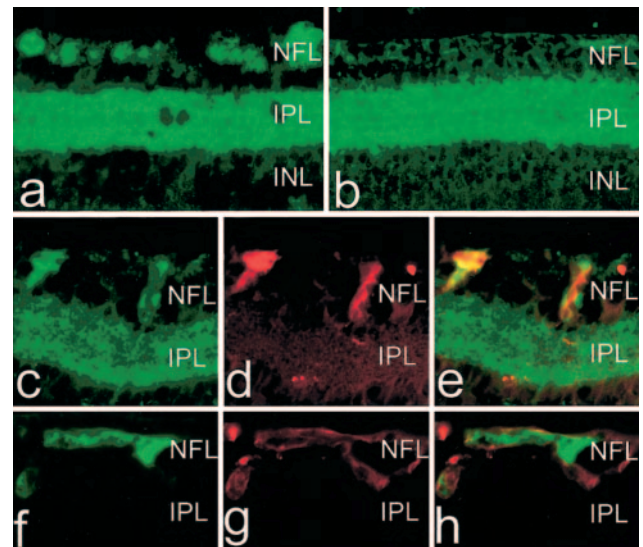


**Figure 3.** COX-2 (a through c, e) and EP<sub>3</sub> (f and h) immunohistochemistry of posthyperoxic (ischemic; a, c through e, f through h) and normoxic mouse retina at P14 (as described in Figure 2); shown are GFAP immunoreactivity (astrocyte marker, d) and lectin griffonia simplicifolia labeling (endothelium marker, g). Panel height, 130  $\mu$ m (a and b); 95  $\mu$ m (c through e); and 48  $\mu$ m (f through h). NFL indicates nerve fiber layer; INL and IPL, inner nuclear layer and inner plexiform layer, respectively.

or the intraretinal revascularization of the ischemic retina studied 4 days after the first dose (P17) (Figure 4A and 4B). However, intravitreal neovascularization (revealed by intravitreal vascular nuclear counts) was dose-dependently diminished by APHS, whereas the selective COX-1 inhibitor SC-560<sup>15</sup> was ineffective (Figure 4C). PGE<sub>2</sub> levels in whole retina were reduced by 65% 24 hours after APHS treatment. Moreover, intravitreal injection of PGE<sub>2</sub> after the hyperoxic period led to a significant (albeit mild) increase in intravitreal neovascularization.

To confirm the role of COX-2 in retinal neovascularization, its involvement was tested using a distinct selective COX-2 inhibitor, etodolac,<sup>16</sup> as well as a different species, the rat model of ischemic proliferative retinopathy. Etodolac caused a marked decrease in retinal neovascularization (studied at 5 days after the first injection) (Figure 5A and 5B). This effect was reversed by PGE<sub>2</sub>.

To further explore the PGE<sub>2</sub> pathway, PGE<sub>2</sub> receptor expression and its changes during the posthyperoxia period were studied. Hyperoxia caused a slight decrease in EP<sub>4</sub> (Figure 5C), whereas EP<sub>1</sub> was undetectable (not shown). In contrast, EP<sub>2</sub> and to a greater extent EP<sub>3</sub> receptor expression was significantly decreased by hyperoxia and increased substantially during the posthyperoxia period (Figure 5C), coincidental with COX-2 changes (Figure 2C). Moreover, addition of the EP<sub>2</sub> agonist butaprost and the EP<sub>3</sub> agonist M&B28767<sup>17</sup> reversed in part or exacerbated the inhibitory effects of etodolac on retinal neovascularization. EP<sub>3</sub> receptor expression also increased in the same phase in that of the murine eye, predominantly localized in retinal endothelium (lectin griffonia-positive cells) (Figure 3f through 3h).

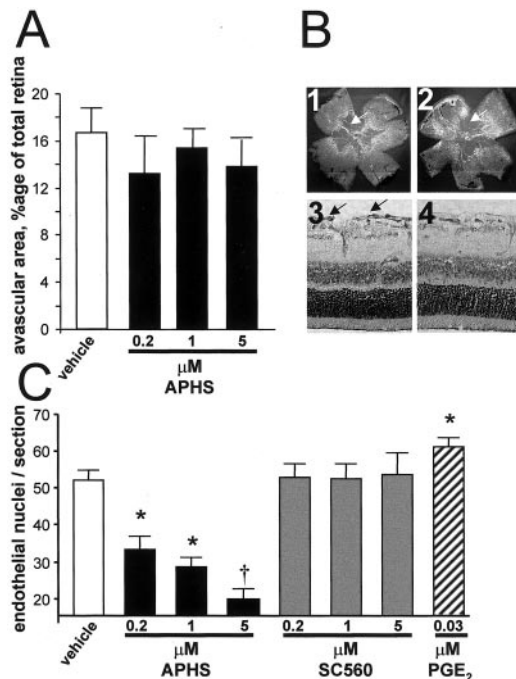


**Figure 4.** Effects of COX-1 and -2 inhibition on retinal vascular density (A and B) and intravitreal neovascularization in murine model of ischemic proliferative retinopathy at P17. Animals were prepared as described in Methods and injected intravitreally at P13 and at P15 with APHS, SC560, or PGE<sub>2</sub>; estimated effective vitreal concentrations are indicated.<sup>15,16</sup> B, Arrows on retinal flat mounts in panels 1 and 2 point to avascular zone and in panel 3 to intravitreal neovessels. Panel heights, 5 mm (B1 and B2) and 240  $\mu$ m (B3 and B4). Values in histograms are mean  $\pm$  SEM; \* $P$ <0.01 compared with vehicle; † $P$ <0.05 compared with other corresponding values for APHS (ANOVA).

### Effects of COX-2 Inhibition and EP<sub>3</sub> Stimulation on Expression of Modulators of Angiogenesis

Involvement of COX-2 and EP<sub>3</sub> on pro- and antiangiogenic factors, notably VEGF, VEGFR2, TSP-1, and CD36,<sup>26,27</sup> was studied in retina of models of proliferative retinopathy. Twenty-four hours after removal from hyperoxia, there was an increase in TSP-1 expression. The COX-2 inhibitor etodolac induced a substantial increase in both TSP-1 and CD36, and addition of the EP<sub>3</sub> agonist M&B28767 reversed this effect. In contrast, effects of COX-2 on neovascularization could not be explained by the VEGF pathway; VEGF expression, although as anticipated it increased during the posthyperoxic period, was marginally affected by etodolac and M&B28767 (Figure 6A), and VEGFR2 remained unaltered. In accord with *in vivo* observations, etodolac caused a slight increase in TSP-1 expression in neuroretinovascular endothelial cells, and this effect was reversed by M&B28767 (Figure 6B), consistent with EP<sub>3</sub> expression on retinal endothelium (Figure 3f).

### Discussion

Inflammatory mediators contribute to the pathogenesis of ischemic proliferative retinopathy.<sup>3,4</sup> In a related manner, COX-2 has been implicated in angiogenesis, especially of tumors.<sup>6</sup> Although COX inhibition diminishes retinal neovascularization in ischemic models,<sup>28</sup> the specific involvement of

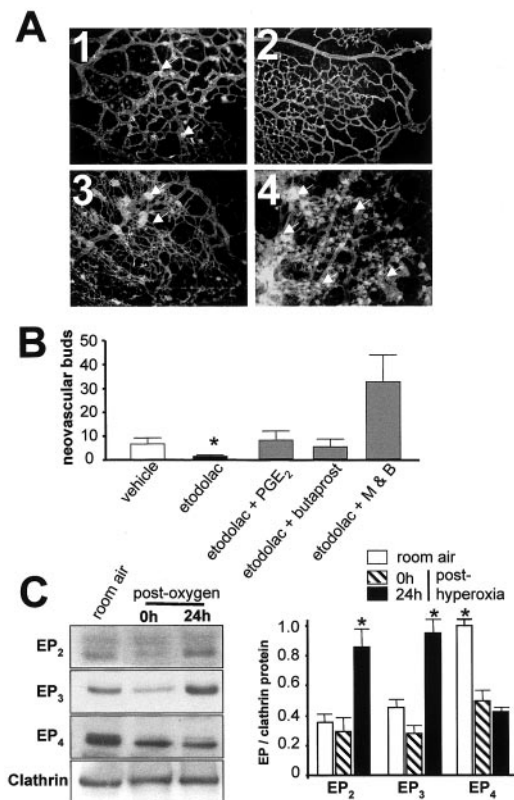


**Figure 5.** Effects of COX-2 inhibitor etodolac and PGE<sub>2</sub> analogs in rat model of ischemic proliferative retinopathy. Rats were exposed to hyperoxia from P1 through P7 (as defined in Figure 2 legend) and injected intravitreally on P7 and P9 with etodolac with or without PGE<sub>2</sub>, butaprost, or M&B28767 (M&B) for estimated effective<sup>16,17</sup> vitreal concentrations, respectively, of 1, 0.1, 10, and 0.1  $\mu$ mol/L; retinas were isolated on P12. A, Retinal flat mounts; 1, vehicle treated; 2, etodolac treated; 3, etodolac+PGE<sub>2</sub> treated; and 4, etodolac+M&B28767 treated. Arrows indicate neovascular buds. Panel height, 1.1 mm. B, EP<sub>2</sub>, EP<sub>3</sub>, and EP<sub>4</sub> protein expression in retinas. Values in histograms are mean  $\pm$  SEM; \* $P$ <0.05 compared with all other corresponding values.

COX-2 and the identity of its products in this process have not been elucidated. Our findings disclose an important role for this immediate-early gene product in proliferative retinopathy. COX-2 expression increased coincidentally with that of EP<sub>2</sub> and EP<sub>3</sub> during the ischemic (posthyperoxic in models) phase associated with proliferation, particularly localized, respectively, in astrocytes and in endothelial cells of the NFL. COX-2 contributed to the preretinal neovascularization in different models of ischemic retinopathies, which seems to be mediated by PGE<sub>2</sub> acting via EP<sub>2</sub> and to a greater extent EP<sub>3</sub> receptors, and these in turn modulate the antiangiogenic factor TSP-1 and its receptor CD36 on target endothelial cells.

COX-2 was abundantly present in synaptic regions of the retina of all species studied (human, mouse, and rat) as seen in the brain.<sup>29</sup> In addition, COX-2 was induced in the NFL of retinas of humans with diabetes and vascular obstruction (case 12) and in animals after hyperoxia, hence during hypoxic-ischemic phases; in these instances, COX-2 was mostly induced in astrocytes (but also in endothelium [Figure

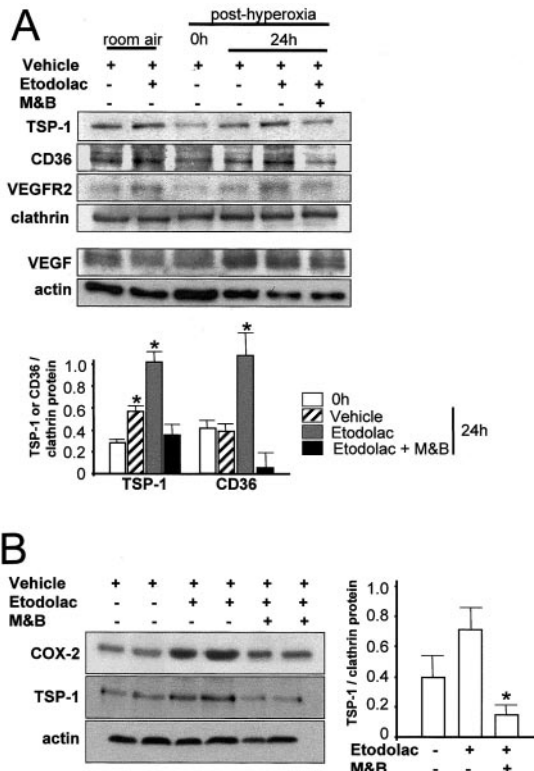


**Figure 6.** A, TSP-1, CD36, VEGFR2, and VEGF expression in rats exposed to room air and after hyperoxia (80% O<sub>2</sub>). Rats were prepared as described in Figure 2. B, COX-2 and TSP-1 immunoreactivity in cultured retinovascular endothelial cells (see Methods) untreated or treated with etodolac (1  $\mu$ mol/L) in presence of M&B28767 (M&B, 0.1  $\mu$ mol/L) or not. Values in histograms are mean  $\pm$  SEM. \* $P$  < 0.01 compared with all other corresponding values.

6B]) and seemed to account for a large portion of PGE<sub>2</sub> generation (Figure 2E). Consistent with the time-dependent and propitious localization of COX-2, molecularly distinct inhibitors of this enzyme (APHS and etodolac<sup>15,16</sup>) markedly diminished preretinal neovascularization (Figures 4 and 5), whereas COX-1 inhibition was ineffective. Moreover, administration of the well-recognized proangiogenic COX product PGE<sub>2</sub><sup>2,5,10</sup> (Figure 4) reversed the antiangiogenic effects of COX-2 inhibitors in the retina (Figures 4 and 5). In view of the significant COX-1 expression even during the hypoxic phase (Figure 2C and 2D), one would have predicted some effect of COX-1 inhibition on neovascularization. However, COX-2 seems to be coregulated and biochemically coupled with the inducible gene product microsomal PGE<sub>2</sub> synthase, a dominant generator of PGE<sub>2</sub> under certain inflammatory conditions,<sup>30</sup> whereas COX-1 appears to be mostly coupled to the constitutive cytosolic PGE<sub>2</sub> synthase. This inference may explain at least in part the differences observed between COX-1 and COX-2 inhibitors. Of note, we found augmented microsomal PGE<sub>2</sub> synthase during the posthyperoxic period (data not shown) and, accordingly, a major role for COX-2 in PGE<sub>2</sub> generation during hypoxia (Figure 2E).

The angiogenic effect of PGE<sub>2</sub> seemed to be mediated via its EP<sub>2</sub> and especially EP<sub>3</sub> receptors, as specific stimulation of these receptors reversed the effects of etodolac on neovascu-

larization (Figure 5); selective antagonists to these receptors are not readily available. Of interest, EP<sub>2</sub> and EP<sub>3</sub> have recently been reported to participate in colorectal tumor angiogenesis,<sup>31,32</sup> and these effects may be mediated via VEGF, a major factor in ischemic proliferative retinopathy<sup>26</sup>; similarly, COX-2 inhibition downregulated VEGF in colon tumor endothelial cells.<sup>8</sup> But in other endothelial cells (breast tumor and cornea), COX-2 inhibition affected the basic fibroblast growth factor pathway,<sup>9</sup> which plays a minor role in ischemic proliferative retinopathy.<sup>33</sup> Endothelial cells are not homogeneous throughout tissues, and in retina the effect of COX-2 inhibition was largely unrelated to the VEGF pathway (Figure 6). Thus, COX-2 inhibition may interfere with pathways that are independent of specific growth factors. Plausible candidate pathways are through TSP-1 and its receptor CD36, which inhibit angiogenesis via p38 mitogen-activated protein kinase and caspase 3.<sup>34</sup> This conjecture is supported by an upregulation of TSP-1 and CD36 by COX-2 inhibitor and reversal of these effects by EP<sub>3</sub> stimulation (Figure 6). Although a prostaglandin D<sub>2</sub> metabolite-dependent peroxisome proliferator-activated receptor- $\gamma$ -mediated induction of TSP-1 and CD36 has been documented,<sup>35</sup> an EP<sub>3</sub>-evoked one as we observed (Figure 6) discloses a previously undescribed mode of regulation of these antiangiogenic factors.

In summary, COX-2 contributes markedly to preretinal neovascularization in ischemic retinopathies, and this effect seems to be PGE<sub>2</sub> mediated mostly via EP<sub>3</sub> receptors implicating a new interaction through TSP-1 and CD36. Results suggest that selective COX-2 inhibitors could be used for the control of pathological vitreal neovascularization in ischemic proliferative retinopathy. More specifically, EP<sub>3</sub> (and possibly EP<sub>2</sub>) antagonists may be more selective by sparing the potentially physiologically desirable effects of the various COX-2 products.

## Acknowledgments

This work was supported by grants from the Canadian Institutes of Health Research, Fond de la Recherche en Santé du Québec (Réseau Vision), March of Dimes, and Heart and Stroke Foundation of Québec. Drs Sennlaub and Beauchamp are supported by fellowships from the Deutscher Akademischer Austauschdienst and the Canadian Institutes of Health Research, respectively. Dr Chemtob holds a Canada Research Chair. We thank Hendrika Fernandez for skillful technical assistance.

## References

- Lee P, Wang CC, Adamis AP. Ocular neovascularization: an epidemiologic review. *Surv Ophthalmol*. 1998;43:245–269.
- Tolentino MJ, Adamis AP. Angiogenic factors in the development of diabetic iris neovascularization and retinopathy. *Int Ophthalmol Clin*. 1998;38:77–94.
- Barouch FC, Miyamoto K, Allport JR, et al. Integrin-mediated neutrophil adhesion and retinal leukostasis in diabetes. *Invest Ophthalmol Vis Sci*. 2000;41:1153–1158.
- Sennlaub F, Courtois Y, Goureau O. Inducible nitric oxide synthase mediates the change from retinal to vitreal neovascularization in ischemic retinopathy. *J Clin Invest*. 2001;107:717–725.
- Sennlaub F, Courtois Y, Goureau O. Inducible nitric oxide synthase mediates retinal apoptosis in ischemic proliferative retinopathy. *J Neurosci*. 2002;22:3987–3993.
- Dubois RN, Abramson SB, Crofford L, et al. Cyclooxygenase in biology and disease. *FASEB J*. 1998;12:1063–1073.



7. Degi R, Thore C, Bari F, et al. Ischemia increases prostaglandin H synthase-2 levels in retina and visual cortex in piglets. *Graefes Arch Clin Exp Ophthalmol*. 2001;239:59–65.
8. Tsujii M, Kawano S, Tsuji S, et al. Cyclooxygenase regulates angiogenesis induced by colon cancer cells. *Cell*. 1998;93:705–716.
9. Masferrer JL, Leahy KM, Koki AT, et al. Antiangiogenic and antitumor activities of cyclooxygenase-2 inhibitors. *Cancer Res*. 2000;60:1306–1311.
10. Leahy KM, Ornberg RL, Wang Y, et al. Cyclooxygenase-2 inhibition by celecoxib reduces proliferation and induces apoptosis in angiogenic endothelial cells in vivo. *Cancer Res*. 2002;62:625–631.
11. Liu XH, Kirschenbaum A, Lu M, et al. Prostaglandin E2 induces hypoxia-inducible factor-1 $\alpha$  stabilization and nuclear localization in a human prostate cancer cell line. *J Biol Chem*. 2002;277:50081–50086.
12. Jones MK, Wang H, Peskar BM, et al. Inhibition of angiogenesis by nonsteroidal anti-inflammatory drugs: insight into mechanisms and implications for cancer growth and ulcer healing. *Nat Med*. 1999;5:1418–1423.
13. Smith LE, Wesolowski E, McLellan A, et al. Oxygen-induced retinopathy in the mouse. *Invest Ophthalmol Vis Sci*. 1994;35:101–111.
14. Holmes JM, Duffner LA. The effect of postnatal growth retardation on abnormal neovascularization in the oxygen exposed neonatal rat. *Curr Eye Res*. 1996;15:403–409.
15. Kalgutkar AS, Crews BC, Rowlinson SW, et al. Aspirin-like molecules that covalently inactivate cyclooxygenase-2. *Science*. 1998;280:1268–1270.
16. Riendeau D, Percival MD, Boyce S, et al. Biochemical and pharmacological profile of a tetrasubstituted furanone as a highly selective COX-2 inhibitor. *Br J Pharmacol*. 1997;121:105–117.
17. Abramovitz M, Adam M, Boie Y, et al. The utilization of recombinant prostanoid receptors to determine the affinities and selectivities of prostaglandins and related analogs. *Biochim Biophys Acta*. 2000;1483:285–293.
18. Beauchamp MH, Marrache AM, Hou X, et al. Platelet-activating factor in vasoobliteration of oxygen-induced retinopathy. *Invest Ophthalmol Vis Sci*. 2002;43:3327–3337.
19. Hou X, Gobeil F Jr, Peri K, et al. Augmented vasoconstriction and thromboxane formation by 15-F(2t)-isoprostane (8-iso-prostaglandin F(2 $\alpha$ )) in immature pig periventricular brain microvessels. *Stroke*. 2000;31:516–525.
20. Dehouck MP, Meresse S, Delorme P, et al. An easier, reproducible, and mass-production method to study the blood-brain barrier in vitro. *J Neurochem*. 1990;54:1798–1801.
21. Marrache AM, Gobeil F Jr, Bernier SG, et al. Proinflammatory gene induction by platelet-activating factor mediated via its cognate nuclear receptor. *J Immunol*. 2002;169:6474–6481.
22. Hardy P, Abran D, Li DY, et al. Free radicals in retinal and choroidal blood flow autoregulation in the piglet: interaction with prostaglandins. *Invest Ophthalmol Vis Sci*. 1994;35:580–591.
23. Benjamin LE, Hemo I, Keshet E. A plasticity window for blood vessel remodelling is defined by pericyte coverage of the preformed endothelial network and is regulated by PDGF-B and VEGF. *Development*. 1998;125:1591–1598.
24. Iadecola C, Niwa K, Nogawa S, et al. Reduced susceptibility to ischemic brain injury and N-methyl-D-aspartate-mediated neurotoxicity in cyclooxygenase-2-deficient mice. *Proc Natl Acad Sci USA*. 2001;98:1294–1299.
25. Form DM, Auerbach R. PGE<sub>2</sub> and angiogenesis. *Proc Soc Exp Biol Med*. 1983;172:214–218.
26. Aiello LP, Pierce EA, Foley ED, et al. Suppression of retinal neovascularization in vivo by inhibition of vascular endothelial growth factor (VEGF) using soluble VEGF-receptor chimeric proteins. *Proc Natl Acad Sci U S A*. 1995;92:10457–10461.
27. Suzuma K, Takagi H, Otani A, et al. Expression of thrombospondin-1 in ischemia-induced retinal neovascularization. *Am J Pathol*. 1999;154:343–354.
28. Takahashi K, Saishin Y, Mori K, et al. Topical nepafenac inhibits ocular neovascularization. *Invest Ophthalmol Vis Sci*. 2003;44:409–415.
29. Kaufmann WE, Worley PF, Pegg J, et al. COX-2, a synaptically induced enzyme, is expressed by excitatory neurons at postsynaptic sites in rat cerebral cortex. *Proc Natl Acad Sci U S A*. 1996;93:2317–2321.
30. Brock TG, McNish RW, Peters-Golden M. Arachidonic acid is preferentially metabolized by cyclooxygenase-2 to prostacyclin and prostaglandin E<sub>2</sub>. *J Biol Chem*. 1999;274:11660–11666.
31. Seno H, Oshima M, Ishikawa TO, et al. Cyclooxygenase 2- and prostaglandin E(2) receptor EP(2)-dependent angiogenesis in Apc(Delta716) mouse intestinal polyps. *Cancer Res*. 2002;62:506–511.
32. Amano H, Hayashi I, Endo H, et al. Host prostaglandin E(2)-EP3 signaling regulates tumor-associated angiogenesis and tumor growth. *J Exp Med*. 2003;197:221–232.
33. Ozaki H, Okamoto N, Ortega S, et al. Basic fibroblast growth factor is neither necessary nor sufficient for the development of retinal neovascularization. *Am J Pathol*. 1998;153:757–765.
34. Jimenez B, Volpert OV, Crawford SE, et al. Signals leading to apoptosis-dependent inhibition of neovascularization by thrombospondin-1. *Nat Med*. 2000;6:41–48.
35. Feng J, Han J, Pearce SF, et al. Induction of CD36 expression by oxidized LDL and IL-4 by a common signaling pathway dependent on protein kinase C and PPAR- $\gamma$ . *J Lipid Res*. 2000;41:688–696.